ENERGY AND EXERGY ANALYSIS INSIDE A TRAPEZOIDAL SOLAR CHIMNEY FROM SHIPPING CONTAINERS TO IMPROVE THERMAL COMFORT

Felipe Person Malta, fpmalta@usp.br[1]
Cyro Albuquerque Neto, cyroan@fei.edu.br[2]
Silvio de Oliveira Júnior, soj@usp.br[1]
Jurandir Itizo Yanagihara, jiy@usp.br[1]

[1]Escola Politécnica da Universidade São Paulo, Av. Prof. Mello Moraes, 2231 - São Paulo - SP
[2]Centro Universitário da FEI, Av. Humberto de Alencar Castelo Branco, 3972-B - São Bernardo do Campo - SP

Abstract: *Solar chimney is a technique widely used to generate clean energy and/or improve thermal comfort inside buildings. Shipping containers are low cost and suitable to be turned into habitation, but the thermal comfort is impaired. The aim of this paper is to apply exergy balance on a solar chimney, from a shipping trapezoidal container wall, in order to improve the thermal comfort. The energy and exergy balance relates the first law of thermodynamics with exergy efficiency and exergy destroyed. The heat loss due reflection, radiation and convection were very close, ranging from 4 to 8 % of the heat supplied. However, the heat effectively provided to the fluid is much smaller, being the average of 2 %. Meanwhile, the heat lost by the insulation is very low and may even be considered negligible. The exergy destroyed, that has a behavior of quadratic function, combined with the behavior of physical exergy, caused a linear decrease of exergetic efficiency of the chimney, the opposite fact to the linear growth in the thermal efficiency. The combination of these two events shows that it would be ideal to use this chimney at a specific point, which would be in balance both efficiencies for optimization of the apparatus.*

Keywords: *Solar Chimney, Natural Convection, Exergy Analysis, Shipping Container, Thermal Comfort.*

1. INTRODUCTION

Shipping containers are often used as a low cost solution for offices, stores and dwellings. Shipping containers are extremely strong structures, made to transport heavy loads around the world. Because of rules of safety, they have a lifetime of twenty years. After that, they must be discarded and can not be loaded again, even if the structure is perfect. Because of that, during the last decades, the humanity is looking for new possibilities of use. The use as habitation is becoming more usual, specially because of the sustainability. Containers are big weathering steel boxes, resistant to corrosion. However, they are also excellent thermal conductors, making it one of the major difficulties found in applications is to maintain the temperature in a comfort range.

Being a simple and practical idea, the technology of solar chimney has been regarded as an attractive bioclimatic design. Solar chimney is a thermo-syphoning air channel in which the principal driving mechanism of air flow is through thermal buoyancy. It utilizes solar radiation to enhance the natural ventilation in buildings, which is achieved as a result of the fact that the solar energy causes a temperature rise as well as a density drop in the air inside the solar chimney. The drop in air density causes air within the solar chimney to rise and be expelled out of the top of the chimney. (Zhai *et al.*, 2011)

In the north hemisphere, the major problem is the cold, so the basic solution is a good insulation and heating system (Fig. 1 right side), while in tropical countries, the most common solution is the use of isolation and air conditioning system (Fig. 1 left side). In this case, the electricity is a vital part of the system and also a expansive solution in terms of energy. Once there are a huge amount of energy from natural sources like the sun and wind, passive techniques can be used to help solving the comfort problem. One of most effective solution is the use of cross ventilation, but we can not rely on it all the time. To increase structural strength, the container wall is shaped like trapezoids. The idea of this work is to study the possibility of creating cavities with this wall and use them as solar chimneys.

The behavior of the air in a solar chimney was the object of study of many authors. The main difference between their chimneys and the one proposed in the present work is the trapezoidal cross section. In all the works found, the cavity cross section is rectangular and bigger. Chen *et al.* (2003) experimentally studied the behavior of a solar chimney varying the size and the inclination of the cavity, with constant heat flux. Arce *et al.* (2009) studied a solar chimney in a external environment, heated by the sun. Sandberg and Moshfegh (1996) were one of the first authors to study a vertical solar chimney. They found that the air flow is larger if the outlet of the chimney is upwardly open, and not laterally, as used in real situation to protect from rain. Moshfegh and Sandberg (1996) also developed numerical simulations.

This technique was also used in other studies. Gan (1998) showed with simulations that the chimney works best if the part to the internal environment is thermally isolated. Bassiouny and Koura (2008) included in their numerical model the internal environment, with a window in the opposite side. Bansal *et al.* (1993) developed a steady-state mathematical model for a roof solar chimney system, consisting of a solar air heater connected to a conventional chimney. Mathur *et al.* (2006) evaluates the increase of the ventilation rate with the increase of the ratio between hight of absorber and gap

Figura 1: **Behavior of a solar chimney in the summer and in the winter.**

between glass and absorber, in agreement with Bansal *et al.* (1993). Ong (2003) and Ong and Chow (2003) investigate the performance of a solar chimney and proposed a simple mathematical model to describe its behavior, but with a glazing wall to receive the radiation and a blackened inner surface to absorb and retain the heat for later use. Burek and Habeb (2007) ascertain the correlation between the channel depth with the mass flow rate and the heat input, but also concluded that the thermal efficiency was only a function of the heat input, and not a dependent of the channel depth.

2. EXPERIMENTAL INVESTIGATION

The experiments were developed in four different days, with the temperature inside the laboratory varied from 294.1 to 296.8 K on these days. The instrumentation was chosen to obtain the main data that describe the behavior of the natural convection inside the chimney. In order to simulate the heat provided by the sun, vertical electric heaters were used. This research is a improvement of the experiment led by Malta *et al.* (2014).

A global view of the experimental apparatus is showed on Fig. (2a). The apparatus was covered (in the back) with an insulation material (expanded polyethylene, Neopor®, BASF) to minimize the heat losses to the ambient. The metallic wall have 2.3 m of height. The inlet and outlet of the cavity are trapezoidal sections with the base equal to 208 mm, the top equal to 72 mm, and a height of 36 mm. The section area is equal to 5040 mm^2 (Fig. (2b)).

(a) Experimental apparatus and sensor locations.

(b) Cavity trapezoidal section.

Figura 2: **Overview of the experimental apparatus and its cross section area. (Measures in milimeters)**

The generation of heat through the metallic wall was made with four cylindrical electric heaters (Elbac), each with the length of 2.2 m and 9 mm of diameter, controlled by a potentiometer. The heaters were fixed by ceramic supports, positioned 0.2 m away from the experiment metallic wall. Six situations were measured with different heat fluxes, close to the highest solar incidence on the surface of the earth.

The container has a beam over the wall, which was included in the experimental apparatus. The beam might be used to protect the cavity from rain. The air inlet should also be horizontal, because it is close to the internal floor.

The temperature and the air velocity were measured in several points of the cavity; Figure 2a shows their positions. To obtain the temperature profile inside the cavity, a type K thermocouple (accuracy of ± 2.2 °C) was set through the insulation, and moved between the internal walls. The air temperatures in the inlet and outlet were also measured. The external temperatures were measured in several points with an infrared thermometer (Fluke 62max+, accuracy of ± 1 °C).

The air velocity inside the cavity was measured in the same height (Fig 2a), with the probe (Testo 405-V1, accuracy of 0.1 m/s + 5 % of the measured value) passing through the insulated wall in three positions, from the center to the left. The right side was considered to have the same velocities, due to the symmetry of the geometry. The probe was moved between the hot and the insulated wall. Each measured point was considered to represent an area, so the average velocity was calculated. With the average velocity, the mass flow was calculated with the temperature measured in that place. All measures were taken after the outlet temperature was stabilized, so the experiment can be considered at steady state.

3. MATHEMATICAL MODEL

The energy balance is necessary to determine the energy efficiency of the chimney, a parameter to indicate quantitatively the usefulness of the experiment. However, it is necessary to measure the quality of the heat transfer, indicated by the exergy efficiency. In this section is described both balances: energetic and exergetic, with all correlations needed to adequate the model and the experiment.

3.1 Energy Balance

The proposed energy balance correlates the measured temperatures with the heat and losses by insulation, borders (without insulation), geometry form factor, reflection, and mainly the dissipation through the air. The heat generation produced by the electrical resistances was calculated using electrical power correlations shown in Eq. (1), given the power result multiplying the electric resistance (R) and electric current (I), measured in Watts.

$$P = RI^2 \tag{1}$$

This heat source is considered a black body, i.e. no losses related due its emissivity. Nevertheless it is necessary to add up another variable to the main equation because mostly of the heat do not reach the metallic wall, as the heat waves are radials (due to the cylindrical heaters) and not unidirectional, i.e. the geometry and the surface orientation have a strong dependance. Therefore, the geometry form factor ($\Im_{01}$) was added to the heat transfer and its analytical solution can be presented in Eq. (2), as a correlation between infinite plate and row of cilynders (Rohsenow $et\ al.$, 1998).

$$\Im_{01} = 1 - \left[1 - \left(\frac{D}{s}\right)^2\right]^{1/2} + \left(\frac{D}{s}\right) tan^{-1}\left[\left(\frac{s^2 - D^2}{D^2}\right)^{1/2}\right] \tag{2}$$

where D is the diameter and s the distance between two cilynders.

The heat transferred to the metallic plate ($\dot{Q}^0$) was considered as the electrical power times the form factor, while the remainder ($\dot{Q}^0_{diss}$) was presumed as heat dissipated into the air and room environments. Part of $\dot{Q}^0$ is reflected to the environment ($\dot{Q}^0_{rf}$) due the non-black surface, i.e. its emissivity (ϵ_w) < 1. In the meantime, the geometry form factor ($\Im_{10}$) it is equal to 1 because the surface sees all of the heat source. The energy balance is summarized in Eq. (3).

$$\dot{Q}^0 = \dot{Q}^0_{rf} + \dot{Q}^1_k + \dot{Q}^1_{\Im_{12}} \tag{3}$$

with $\dot{Q}^1_k$ the conduction heat transfer and $\dot{Q}^1_{\Im_{12}}$ the heat loss due form factor.

The heat absorption warms the plate, increasing its temperature above the environment temperature, causing two phenomena: radiation ($\dot{Q}^0_{rad}$) and convection ($\dot{Q}^0_{conv}$) heat transfer to the external environment. To the radiation, the form factor is equal to 1 and its emissivity is $\epsilon_w = 0.97$. The convection heat transfer (h^0_∞) needs to be determined, using empirical or experimental correlations. Awbi (1998) ascertain a correlation between h_∞, hydraulic diameter (D_H), and temperature difference in a room and its vertical wall, with low velocity fluid, shown in Eq. (4). Equation (5) shows the radiation and Eq. (6) the convection heat transfer.

$$h^0_\infty = 1.823 \left[\frac{(T^0_w - T^0_\infty)^{0.293}}{(D^0_{H_w})^{0.121}}\right] \tag{4}$$

$$\dot{Q}^0_{rad} = \sigma A^0_w \epsilon_w \left[\left(T^0_w\right)^4 - \left(T^0_\infty\right)^4 \right] \tag{5}$$

$$\dot{Q}^0_{conv} = A^0_w h^0_\infty \left(T^0_w - T^0_\infty\right) \tag{6}$$

where σ is the Boltzmann constant, A^0_w the external surface area of the heated wall, T^0_w the external temperature of the wall, T^0_∞ the air and wall temperature of the room, $D^0_{H_w}$ the hydraulic diameter of the external surface heated wall.

It is necessary, due the Eq. (3), to use another form factor equation to quantify the heat loss inside the trapezoidal chimney, shown in Eq. (7). This is caused by the relationship between inside the heated wall surface and inside heated insulation surface.

$$\dot{Q}^1_{\Im_{12}} = \frac{2\sqrt{1 + (f_1)^2} + f_2}{2 + f_2} \tag{7}$$

with $f_1 = \frac{x}{y}$ and $f_2 = \frac{\bar{y}}{y}$ the correlation between the trapezoidal geometry, shown in Fig. (2b).

The following equations (Eq. 8 to 14) ascertain all the energy balance set up for the trapezoidal solar chimney, presented in Fig. (3), with convection and radiation due the heated wall for the inlet air ($\dot{Q}^2_{conv}$ and $\dot{Q}^2_{rad}$), convection and reflection of the heated insulation for the inlet air ($\dot{Q}^3_{conv}$ and $\dot{Q}^3_{rf}$), and conduction to the outside environment ($\dot{Q}^4_k$). The last one was used to define the heat loss, combined with the insulation temperature inside the cavity (T^3_{ins}) and the air temperature of the room (T^0_∞), shown in Eq. (13). To do that, it is necessary to use a correlation between convection and the radiation heat loss to the outside environment due the insulation ($\dot{Q}^5_{conv}$ and $\dot{Q}^5_{rad}$), because the outside insulation temperature was not measured, established Eq. (14).

$$\dot{Q}^1_k = \dot{Q}^2_{conv} + \dot{Q}^2_{rad} \tag{8}$$

$$\dot{Q}^2_{rad} = \dot{Q}^3_{conv} + \dot{Q}^3_{rf} + \dot{Q}^4_k \tag{9}$$

$$\dot{Q}^3_{rf} = \dot{Q}^1_{k_{rf}} \tag{10}$$

$$\dot{Q}^1_{k_{rf}} = \dot{Q}^0_{conv} + \dot{Q}^0_{rad} \tag{11}$$

$$\dot{Q}^4_k = \dot{Q}^5_{conv} + \dot{Q}^5_{rad} \tag{12}$$

$$\dot{Q}^4_k = \frac{\left(T^3_{ins} - T^0_\infty\right)}{t_{ins}(k^4_{ins} A^4_{ins})^{-1} + 0.5485\varphi \left(D^5_{H_{ins}}\right)^{0.121} \left(T^3_{ins} - T^0_\infty\right)^{-0.293} \left(A^5_{ins}\right)^{-1}} \tag{13}$$

$$\varphi = \frac{\dot{Q}^0_{conv}}{\dot{Q}^0_{rad}} = \frac{\dot{Q}^5_{conv}}{\dot{Q}^5_{rad}} \tag{14}$$

with t_{ins}, k^4_{ins}, A^4_{ins}, $D^5_{H_{ins}}$, and A^5_{ins} the thickness, thermal conductivity, internal area, hydraulic diameter, and external area of the insulation, respectively.

Both convection phenomena inside the chimney can be related with the first law of thermodynamics for ideal gases, without work load and the effects of velocity and height neglected due its magnitude compared to the enthalpy difference. Therefore, the convection heats are stated in Eq. (15).

$$\dot{Q}^2_{conv} + \dot{Q}^3_{conv} = \dot{Q}_{fluid} = \dot{m}c_{p_{air}}(T_{out} - T_{in}) \tag{15}$$

The overall correlation of $\dot{Q}^0$ is summarized in Eq. (16). It is possible to discover the reflected (and borders loss) heat $\dot{Q}^0_{rf}$, since all of the heats were calculated with measurable variables.

$$\dot{Q}^0 = \dot{Q}^0_{rf} + \dot{Q}^0_{conv} + \dot{Q}^0_{rad} + \dot{Q}_{fluid} + \dot{Q}^4_k \tag{16}$$

When all heats are measured, it is possible to calculate the energy efficiency, given by the Eq. (17).

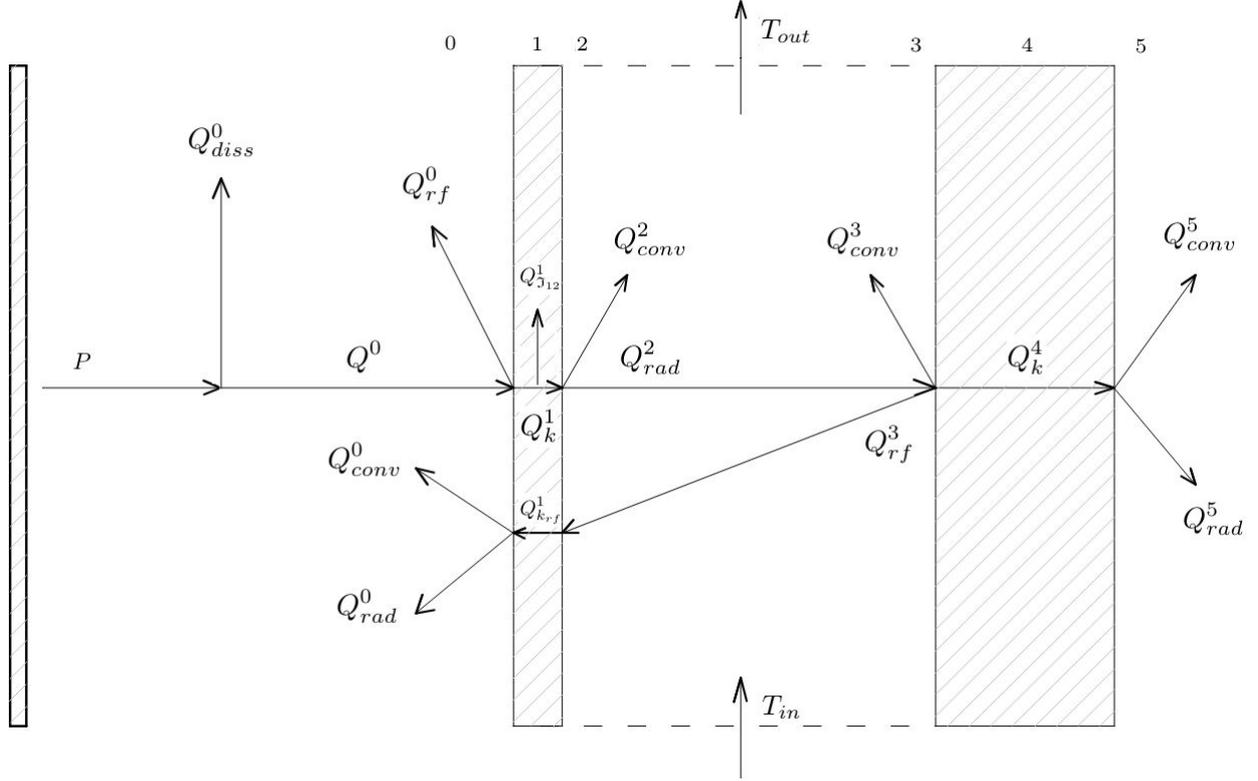$$\eta_T = \frac{\dot{Q}_{fluid}}{\dot{Q}^0} \times 100\% \tag{17}$$

Figura 3: **Energy balance for the trapezoidal solar chimney**

3.2 Exergy Balance

In this paper, a exergy balance is calculated with exergy equations for heat exchanges (at different temperatures), one inlet and outlet section, fixed control volume, and steady state regime. Thereafter the exergy efficiency is computed in order to compare both energy and exergy efficiency.

The control volume analysed enfold the zones 1 to 3, having as exchanged heats $\dot{Q}^0$, $\dot{Q}^0_{rf}$, $\dot{Q}^0_{conv}$, $\dot{Q}^0_{rad}$, $\dot{Q}^1_{\mathfrak{I}_{12}}$, and $\dot{Q}^4_k$, with the mass flow $\dot{m}$ at T_{in} and T_{out}. All exergy flows derived from these heats exchanges are shown in the Eq. (18) to (23).

$$\dot{B}^0 = \Theta_w \dot{Q}^0 \tag{18}$$

$$\dot{B}^0_{conv} = \Theta_w \dot{Q}^0_{conv} \tag{19}$$

$$\dot{B}^0_{rad} = \Theta_w \dot{Q}^0_{rad} \tag{20}$$

$$\dot{B}^0_{rf} = \Theta_w \dot{Q}^0_{rf} \tag{21}$$

$$\dot{B}^1_{\mathfrak{I}_{12}} = \Theta_w \dot{Q}^1_{\mathfrak{I}_{12}} \tag{22}$$

$$\dot{B}^4_k = \Theta_{ins} \dot{Q}^4_k \tag{23}$$

with $\Theta_w = \left(1 - \frac{T^0_\infty}{T^0_w}\right)$ the Carnot factor at wall temperature, $\Theta_{ins} = \left(1 - \frac{T^0_\infty}{T^0_{ins}}\right)$ the Carnot factor at insulation temperature.

The physical exergy provided by the mass flow is established in Eq. (24).

$$\dot{B}_{ph} = \dot{m}\left[c_{p_{air}}(T_{in} - T_{out}) - T^0_\infty c_{p_{air}} ln\left(\frac{T_{in}}{T_{out}}\right) - gH_w\right] \tag{24}$$

with H_w the height of the metallic wall (shown in Fig. (2a)).

Combining these equations in the exergy balance, it is possible to ascertain the exergy destroyed in the experiment (Eq. (25)) and, lastly, quantify its exergetic efficiency (Eq. (26)).

$$\dot{B}_{dest} = \dot{B}^0 - \dot{B}^0_{conv} - \dot{B}^0_{rad} - \dot{B}^0_{rf} - \dot{B}^1_{\mathfrak{I}_{12}} - \dot{B}^4_k + \dot{B}_{ph} \tag{25}$$

$$\eta_{\dot{B}} = \frac{\dot{B}_{ph}}{\dot{B}^0} \times 100\% \tag{26}$$

4. RESULTS AND DISCUSSION

4.1 Energy and Exergy Balance

The heat exchange occurred in the solar chimney is summarized by the Sankey diagram, in Fig. (4). With this, it is possible to visualize how much of each heat transfer have the most effect on the experiment. Clearly the form factor $\Im_{01}$ caused a major loss in the experiment, but this was expected, in order to achieve the received heat transfer in the metallic wall, such as the heat provided by the sun. Because of that, these heat dissipated by the form factor can not be taken as a properly loss in the experiment, because that heat was not expected to reach the metallic plate, but only part of it. In spite of the sun has heat fluctuations across the hole day (with peaks at 11 to 13 pm), this methodology makes it possible to reproduce part of the effect caused by these peaks in the wall, but in a laboratory.
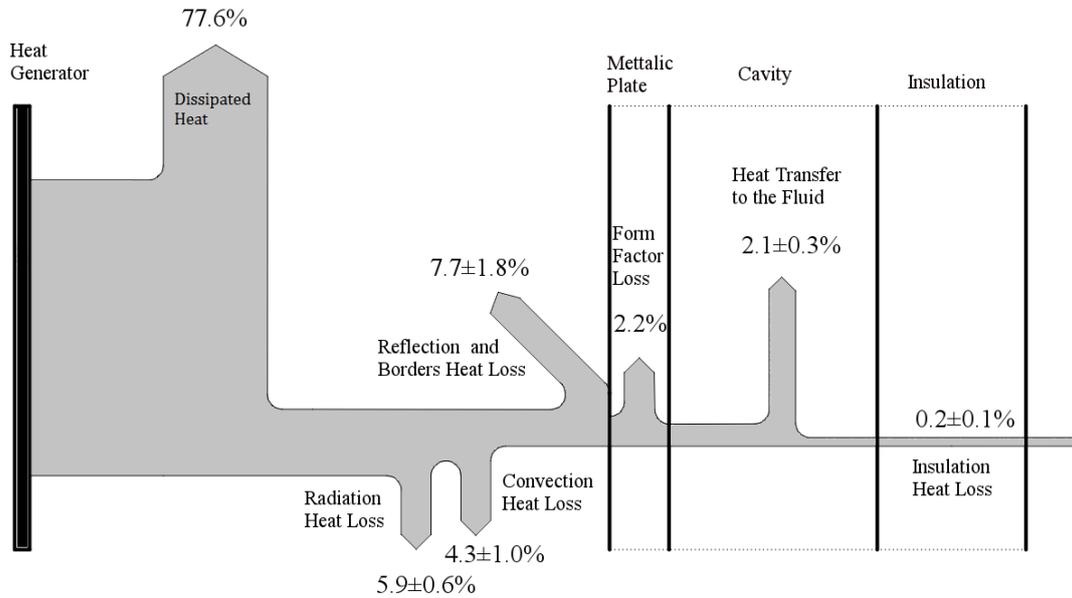
Figura 4: **Energy balance of the solar chimney.**

The heat loss by convection, radiation and through reflection/borders have similar values when compared themselves with the five cases tested, causing a great lost in part of the heat received in the plate only because of that phenomena. Furthermore there is a heat loss caused by the plate form factor ($\Im_{12}$), wich is a relatively high value, since it is very similar to the heat received by the fluid. Nevertheless, the heat lost by the insulation is very small compared to others, but should be computed in the energy balance.

The wall temperatures, input and output are shown in Fig. (5a). It is observed that the wall temperature increases linearly and has an increase of about 23 K over the first temperature obtained. Instead, the outlet temperature was only an increase of 8 K when compared to its first temperature. The losses to the outside air are higher when compared to the effectively heat that is provided to the fluid, impairing the thermal efficiency (causing only a small increase) and making the exergetic efficiency smaller with the increase of power generated.

In terms of exergy, part of the exergy is destroyed in the process due to entropy difference of the fluid, caused by the Eq. (24). Figure (5b) shown the exergy destroyed in the experiment, adjusted by a quadratic equation tendency line with $R^2 = 0.9988$, ranging from 0.05 to 2.4 W. The increase of exergy destroyed in the system is normal, since a larger amount of heat was provided in the experiment, but this quadratic equation impairs the efficiency with a greater extent than the heat to the fluid can compensate. Therefore, these results indicate that increasing the heat received on the plate will cause a higher exergy destroyed, in a way that its exergetic efficiency decreases with the increase of power generated.

Opposite values are perceived in the calculation of the thermal efficiency, noticed due to the increase that exists in the heat received by the fluid, where there is a linear increase as more heat is supplied to the system. The exergetic efficiency varies from 5 to 2.4 %, while energy efficiency ranged from 7.8 to 10 %. Both energetic and exergetic efficiency is demonstrated in Fig. (6), with linear correlations for the two efficiencies. These increase in the energy and decrease in exergy shows a different behavior for the experiment, which is necessary a specific incident power supply to balance both efficiencies in order to achieve optimum results, since the balance of both characteristics is the best setting for the amount of air that can be exchanged throughout the day.

5. CONCLUSION

In this article it was demonstrated energy and exergy balance in a trapezoidal solar chimney for thermal comfort. It is possible to observe that most of the heat generated is lost until it reaches the metallic wall, but this is expected to happen, so that the actual amount of heat arrive on the plate, simulating the heat of the sun. Among the other heats obtained, in
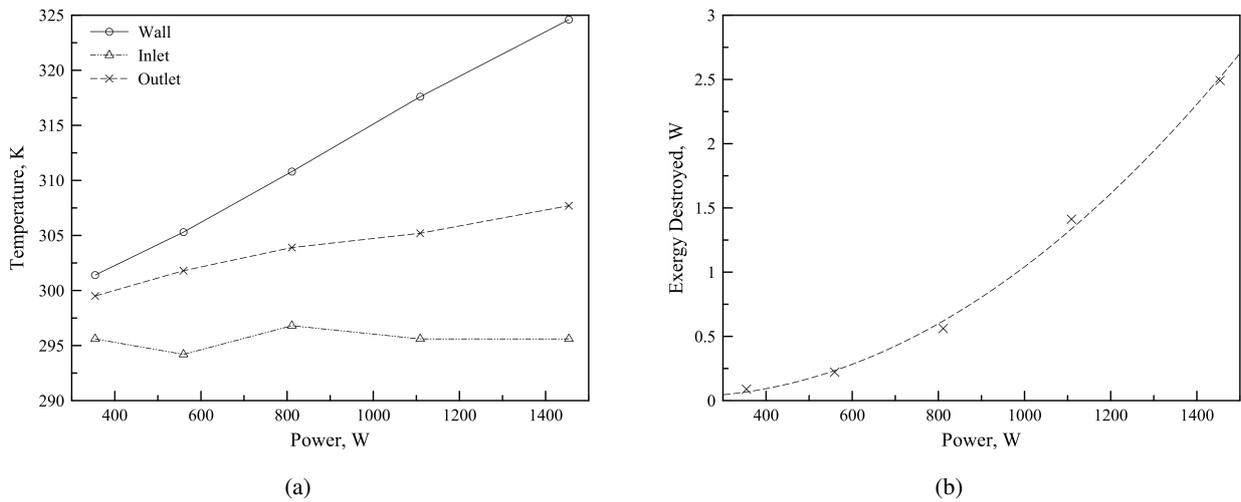
(a)   (b)

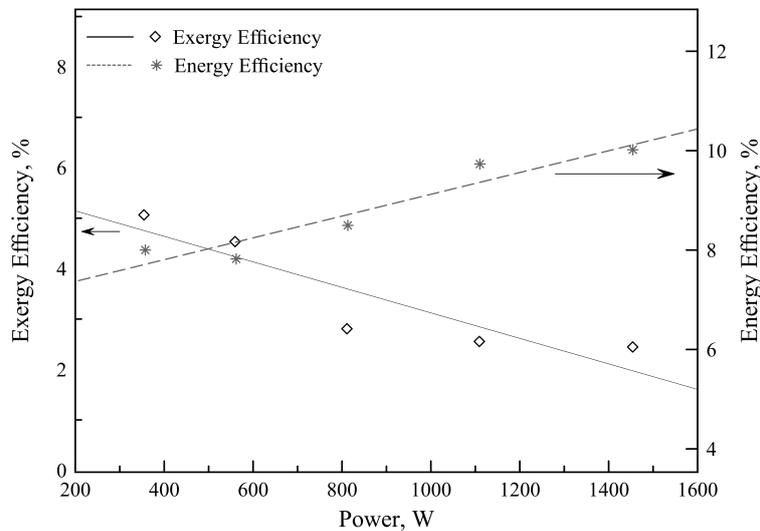Figura 5: **Temperatures of the experiment (a), solar chimney exergy destroyed (b).**

Figura 6: **Energetic and exergetic efficiency of the solar chimney.**

general their values were very close, ranging from 4 to 8 % of the heat supplied. However, the heat effectively provided to the fluid is much smaller, being the average of 2 %. Meanwhile, the heat lost by the insulation is very low and may even be considered negligible. In order to a better attainment of the produced heat flow, a heat flux transducer or piranometer would be desirable.

Regarding the exergetic part, the exergy destroyed, that has a behavior of quadratic function, combined with the behavior of physical exergy, caused a linear decrease of exergetic efficiency of the chimney, the opposite fact to the linear growth in the thermal efficiency. The combination of these two events shows that it would be ideal to use this chimney at a specific point, which would be in balance both efficiencies for optimization of the apparatus.

Despite the heavy losses caused by the apparatus, all energy and exergetic effects would be lost, anyway. Therefore, this solution causes an improvement in thermal comfort at a very low cost, since the container is covered with a thermal insulator to be used as dwelling.

6. ACKNOWLEDGEMENTS

7. REFERENCES

Arce, J., Jiménez, M.J., Guzmán, J.D., Heras, M.R., Alvarez, G. and Xamán, J., 2009. "Experimental study for natural ventilation on a solar chimney". *Renewable Energy*, Vol. 34, No. 12, pp. 2928–2934.

Awbi, H.B., 1998. "Calculation of convective heat transfer coefficients of room surfaces for natural convection". *Energy and Buildings*, Vol. 28, No. 2, pp. 219–227.

Bansal, N., Mathur, R. and Bhandari, M., 1993. "Solar chimney for enhanced stack ventilation". *Building and environment*, Vol. 28, No. 3, pp. 373–377.

Bassiouny, R. and Koura, N.S.A., 2008. "An analytical and numerical study of solar chimney use for room natural ventilation". *Energy and Buildings*, Vol. 40, No. 5, pp. 865–873.

Burek, S. and Habeb, A., 2007. "Air flow and thermal efficiency characteristics in solar chimneys and trombe walls". *Energy and Buildings*, Vol. 39, No. 2, pp. 128–135.

Chen, Z.D., Bandopadhayay, P., Halldorsson, J., Byrjalsen, C., Heiselberg, P. and Li, Y., 2003. "An experimental investigation of a solar chimney model with uniform wall heat flux". *Building and Environment*, Vol. 38, No. 7, pp. 893–906.

Gan, G., 1998. "A parametric study of trombe walls for passive cooling of buildings". *Energy and Buildings*, Vol. 27, No. 1, pp. 37–43.

Malta, F.P., Gouveia, J.L.F. and Albuquerque, C., 2014. "A study of a solar chimney to improve comfort inside shipping containers". In *Proceedings of the 27th International Conference on Efficiency, Cost, Optimization, Simulation and Environmental Impact of Energy Systems*.

Mathur, J., Bansal, N., Mathur, S., Jain, M. *et al.*, 2006. "Experimental investigations on solar chimney for room ventilation". *Solar Energy*, Vol. 80, No. 8, pp. 927–935.

Moshfegh, B. and Sandberg, M., 1996. "Investigation of fluid flow and heat transfer in a vertical channel heated from one side by pv elements, part i - numerical study". *Renewable Energy*, Vol. 8, No. 1, pp. 248–253.

Ong, K.S., 2003. "A mathematical model of a solar chimney". *Renewable energy*, Vol. 28, No. 7, pp. 1047–1060.

Ong, K. and Chow, C., 2003. "Performance of a solar chimney". *Solar energy*, Vol. 74, No. 1, pp. 1–17.

Rohsenow, W.M., Hartnett, J.P., Cho, Y.I. *et al.*, 1998. *Handbook of heat transfer*, Vol. 3. McGraw-Hill New York.

Sandberg, M. and Moshfegh, B., 1996. "Investigation of fluid flow and heat transfer in a vertical channel heated from one side by pv elements, part ii - experimental study". *Renewable Energy*, Vol. 8, No. 1, pp. 254–258.

Zhai, X., Song, Z. and Wang, R., 2011. "A review for the applications of solar chimneys in buildings". *Renewable and Sustainable Energy Reviews*, Vol. 15, No. 8, pp. 3757–3767.

8. RESPONSIBILITY NOTICE

The authors are the only responsible for the printed material included in this paper.